EVOLUTION & DEVELOPMENT 9:6, 527–539 (2007)

Widespread RNA segregation in a spiralian embryo

Evan P. Kingsley,[1] Xin Yi Chan, Yingli Duan, and J. David Lambert*

Department of Biology, University of Rochester, Rochester, NY 14627, USA

*Author for correspondence (email: dlamber2@mail.rochester.edu)

[1]Present address: Department of Organismic and Evolutionary Biology, Harvard University, Cambridge, MA

SUMMARY Asymmetric cell divisions are a crucial mode of cell fate specification in multicellular organisms, but their relative contribution to early embryonic patterning varies among taxa. In the embryo of the mollusc *Ilyanassa*, most of the early cell divisions are overtly asymmetric. During *Ilyanassa* early cleavage, mRNAs for several conserved developmental patterning genes localize to interphase centrosomes, and then during division they move to a portion of the cortex that will be inherited by one daughter cell. Here we report an unbiased survey of RNA localization in the *Ilyanassa* embryo, and examine the overall patterns of centrosomal localization during early development. We find that 3–4% of RNAs are specifically localized to centrosomes during early development, and the remainder are either ubiquitously distributed throughout the cytoplasm or weakly enriched on centrosomes compared with levels in the cytoplasm. We observe centrosomal localization of RNAs in all cells from zygote through the fifth cleavage cycle, and asymmetric RNA segregation in all divisions after the four-cell stage. Remarkably, each specifically localized message is found on centrosomes in a unique subset of cells during early cleavages, and most are found in unique sets of cells at the 24-cell stage. Several specifically localized RNAs are homologous to developmental regulatory proteins in other embryos. These results demonstrate that the mechanisms of localization and segregation are extraordinarily intricate in this system, and suggest that these events are involved in cell fate specification across all lineages in the early *Ilyanassa* embryo. We propose that greater reliance on segregation of determinants in early cleavage increases constraint on cleavage patterns in molluscs and other spiralian groups.

INTRODUCTION

Available evidence suggests that the set of genes involved in early embryonic patterning is highly conserved across the animal kingdom. In contrast, the cellular context of early animal development varies widely among animal embryos. Understanding how the cellular context affects gene function will be important for understanding the mechanisms and evolution of animal development. One cellular process that is particularly important for developmental patterning is the asymmetric partitioning of particular molecules during cell division. This process occurs across the Metazoa, and multicellular eukaryotes in general. Nevertheless, the extent of similarity between taxa in the mechanisms of segregation is not clear.

In the early development of the snail *Ilyanassa* (Fig. 1), mRNAs for several developmental patterning genes are asymmetrically segregated by an apparently novel mechanism (Lambert and Nagy 2002). Each mRNA binds to a particular subset of centrosomes shortly after a division. In the next prophase, the RNA moves from the centrosome to a patch of cortex that will be inherited entirely by one of the daughter cells of the next division. This process, repeated over successive cell divisions, segregates RNAs to sets of cells with similar developmental potentials, suggesting that these cells' fates could be defined, at least in part, by inheritance of centrosomally localized mRNAs. Two observations suggest that localization to the centrosome is a key part of this process. First, in experiments where two interphase centrosomes were introduced into a single common cytoplasm, RNAs localized to the appropriate centrosome, suggesting that the localization is mediated by specific interactions between RNAs and centrosomes. Second, blocking RNA localization to the centrosome by depolymerizing microtubules prevented the subsequent localization to the cortex, leading to apparent degradation of the RNAs that failed to localize (Lambert and Nagy 2002).

Historically, mollusc embryos have been considered to be largely patterned by autonomous cues like segregated determinants. Embryological manipulations provide some support for this. The polar lobe is an anucleate extrusion from the vegetal pole during early cleavages that is inherited by one of the cells at the four-cell stage (Fig. 1). Removal of the lobe blocks normal cell fate specification in the lineage that inherits the lobe material (the D quadrant) and in other cells that require induction by D quadrant cells (Crampton 1896; Clement 1952). Other evidence for autonomous specification in molluscs comes from cell dissociation experiments. The

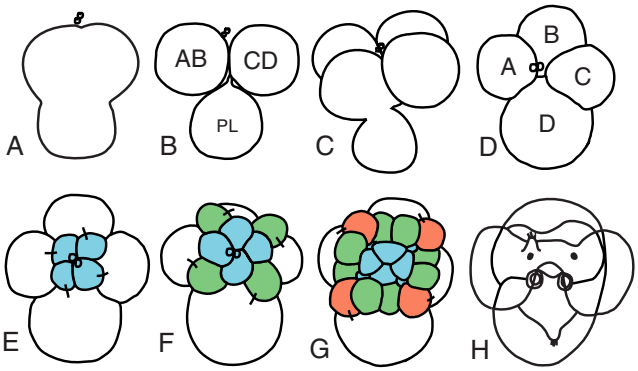

Fig. 1. Early cleavage of *Ilyanassa*. (A–C) Polar lobes are produced at the vegetal pole during the first two cleavages. (D) At the four-cell stage, the cells are named A–D and known as macromeres. The D macromere is larger because it has inherited the polar lobe material. (E–G) In successive cleavage cycles, the macromeres divide synchronously toward the animal pole to produce sets of smaller cells called micromeres. Each set of four micromeres is called a quartet. Hatch marks connect the macromeres to the cells of the quartet born in the preceding stage. (E) The eight-cell stage, after the birth of the first quartet ('1q'). (F) The 12-cell stage, after the birth of the second quartet ('2q'). The first quartet cells will divide next to produce the 16-cell stage. (G) The 24-cell stage follows the birth of the third quartet ('3q'). (H) The veliger larva hatches after about 7 days, with all ectodermal structures derived from the first three quartets of micromeres. Views are from the side in A and B, and from the animal pole in C–G.

trochoblasts produce most of the ciliated band of the larva. When these cells are isolated they carry out the appropriate number of divisions and produce abundant cilia, consistent with their normal course of differentiation (Wilson 1904). On the other hand, it has become clear that signaling in the early embryo is necessary for specification of a variety of lineages (Clement 1962; Sweet 1998; Lambert and Nagy 2001). Hence, while mollusc embryos likely have some lineages that require autonomous cues, it is not yet clear how much of the early embryo is patterned in this way.

A previous study examined the segregation of three RNAs that were cloned by homology to important developmental patterning genes in other organisms. These are the *Ilyanassa* orthologs of the Dpp/BMP2&4 secreted signaling ligand; the Tolloid protease, a regulator of Dpp signaling; and the Even-skipped transcription factor. These three mRNAs were specifically localized to centrosomes and segregated—whereas the mRNA for a ribosomal protein was not—suggesting that RNAs with patterning functions might be preferentially segregated by this mechanism. In this study we report an unbiased survey of the patterns of RNA localization in the early *Ilyanassa* embryo. These data allow us to address several key questions about this phenomenon. We have measured the frequency of specific localization among RNAs, as well as the set of cell lineages where specific localization occurs. Using RNAs recovered in these screens, we have examined the subcellular distribution of localized RNAs during the first five cleavage stages. Finally, we used the sequence of specifically localized RNAs to assess whether they are more likely to encode proteins predicted to play roles in embryonic patterning than the general population of RNAs at these stages. The central conclusion of these analyses is that RNA trafficking in the *Ilyanassa* embryo is exceptionally intricate and extensive, suggesting that these events segregate cues important for cell fate specification in many lineages in the early embryo.

MATERIALS AND METHODS

Snail husbandry

Adult *Ilyanassa obsoleta* were held at 4–8°C in artificial seawater (Instant Ocean, Burlington, NC, USA), until needed for egg laying, when they were moved to tanks at room temperature. Animals were fed frozen clams every other day and embryos were collected as previously described (Collier 1981).

In situ hybridization

Embryos were fixed in 4% or 8% formaldehyde with PEM (100 mM PIPES [pH 6.9], 10 mM EGTA, 1 mM $MgSO_4$, and 0.1% Triton-X 100) and 75–100 mM sucrose for 30–60 min, washed twice in methanol, and stored at −20°C. The cDNA library was constructed from embryos ranging in age from one cell to gastrula (0–48 h) and constructed in the Lambda Zap II vector according to manufacturer's instructions (Stratagene, La Jolla, CA, USA). Probe template was generated by colony PCR with M13F+R primers. For the initial screen (first 113 clones), the PCR reactions were analyzed by electrophoresis, and purified by phenol/chloroform extraction. Probe synthesis was performed using T7 RNA polymerase and Dig-UTP (Roche, Basel, Switzerland) according to manufacturer's protocols. RNA synthesis was confirmed by electrophoresis on standard agarose gels.

For each probe a mix of embryos ranging from oocyte to 24 cells was assembled, and in situ hybridization, 4′,6-diamidino-2-phenylindole (DAPI) staining and mounting was performed as previously described (Lambert & Nagy 2002), except that the hybridization solution contained 5X SSC, 1X Denharts, 50% formamide, 0.1% Tween 20, 100 mg/ml heparin and 100 mg/ml yeast rRNA plus tRNA.

High-throughput in situ screen

The second phase of our screen was carried out in 96-well plates, using modifications to our protocol that were largely based on protocols used by the Berkeley *Drosophila* Genome Project in situ screen project (Tomancak et al. 2002). Embryos were rehydrated in nine-well glass dishes, then moved to 96-well plates. We used plates with porous membrane floors (part number MADVN65, Millipore, Billerica, MA, USA), and a vacuum line attached to a Lucite block with a plate-sized silicone gasket surrounding a well for drainage. Solutions were added using automated eight-channel pipettors, and removed by vacuum. All steps were similar to our standard protocol, excepting the following modifications. We used PCR reactions directly at a 1/3 volume in the probe synthesis reactions, and scaled the synthesis reactions down to 10 µl. We

examined a small subset of the templates and probes by electrophoresis. After hybridization, embryos were washed six times in heated hybridization solution (rather than three times). Also, instead of stopping the alkaline phosphatase developing reaction by washing with PBTw, we stopped each well by adding a 1/10 volume of 1 M EDTA. This allowed us to stop different wells in the plate at different times. Initial visual screening was performed in the plate, at 50 × on a stereomicroscope. In situs with specific localization patterns were removed for further examination at high power. The main technical challenge was avoiding dust accumulation in the wells, as the solution was never pipetted out. When the plates were kept covered during all incubations, and buffer reservoirs were changed frequently, the dust accumulation was minimal.

The RNAs we characterize here from the high-throughput screen were among the first 1410 clones screened using this protocol. The discovery rate of specific localization was lower than in the initial screen. This seems to be a technical artifact; the frequency measured in the initial screen is more reliable, based on our quality control experiments. High-throughput approaches are expected to have higher false-negative and false-positive rates than traditional protocols. To test whether the presumed false-positive rate was due to problems with the 96-well plate in situ, we hybridized the 113 probes of the initial screen in the 96 well plate format. All four of the highly specific RNAs in this set were identified in this experiment, indicating that the in situ hybridization and visual screening steps were not creating false negatives. Subsequent tests, mostly conducted after we stopped screening, indicated that the false negatives were largely caused by unexpectedly high concentrations for some sets of probes, which produced nonspecific background when added at our normal dilution. We repeated the in situs in tubes for all RNAs that appeared to be specifically localized in the 96-well plate screen. These repeat in situs all demonstrated the same specificity of localization as the plate in situs, suggesting that our rate of false positives was zero.

Fluorescent in situs

The fluorescent in situs were carried out as described above for our standard protocol, except for the following. After the probe was washed out, an anti-β tubulin mouse monoclonal antibody (DSHB) was added in PBTw+2%BSA and left on overnight, washed 6 × over 1 h, then anti-DIG POD was added along with anti-mouse Alexafluor 488 (Molecular Probes, Eugene, OR, USA), and incubated overnight. Embryos were washed as before, then detected with tyramide signal amplification using tyramide Cy3 according to manufacturer's instructions (Perkin-Elmer, Waltham, MA, USA), and counter stained and mounted as above.

Microscopy

For each probe in the initial screen, and each putative localized RNA in the high-throughput screen, multiple embryos from each cleavage stage were mounted individually on slides and examined under a 40 × objective on a Zeiss Axioplan II, using DIC and epifluoresence. For in situs in the initial screen that were determined to have nonspecific or no localization, we mounted a large number of embryos on a single slide to verify this assessment. Embryos were photographed using a 6 MP Canon 300D digital SLR camera body attached to the photo tube with a SE16ZK adaptor (Qioptiq, Rochester, NY). The camera was controlled from a PC with Canon Remote Capture software, and the images were downloaded to the hard drive. Fluorescent in situs were examined and documented on a Leica SP confocal. For each image, a Z-series was captured and then projected using Leica software.

Sequencing and analysis

After analysis of the in situs in the initial screen, all clones were sequenced by at least one pass from the putative 5′ end of the directionally cloned insert. When the initial sequencing failed to identify an ortholog with an E value under 0.001 in a blastx search, we sequenced the entire clone (Altschul et al. 1990). For some clones, the first sequencing read covered the clone; for the rest, we ordered internal primers to finish sequencing. All sequences were examined for homology at the nucleotide level using blastn searches, but only one clone, IoEST076 (16S mitochondrial ribosomal RNA), had significant homology in a blastn search that did not correspond to homology at the amino acid level. To find RNAs encoding zinc finger motifs we performed InterProScan motif searches on all sequences (Zdobnov and Apweiler 2001).

RESULTS

The frequency of centrosomal localization

We wanted to know the proportion of RNAs that localize to centrosomes during early cleavage. For 113 clones from a fertilization−gastrulation cDNA library, we made digoxigenin-labeled RNA probes, performed in situ hybridization on early cleavage stages, and examined and documented patterns of RNA distribution. After the patterns were described, we sequenced all clones and found that 10 clones were redundant, so our data set included 103 putatively unique sequences.

Four of 103 unique RNAs have highly specific centrosomal localization, where some or all cells have strong centrosomal localization and little or no cytoplasmic accumulation (Fig. 2A and various panels in Fig. 3). These patterns are considered in depth below. Forty-eight RNAs (47%) had nonspecific localization to centrosomes, where there was significant cytoplasmic accumulation in cells where centrosomal localization occurred (Fig. 2B). Finally, 51 of 103 RNAs exhibited ubiquitous cytoplasmic staining (Fig. 2, C and D). The cytoplasmic staining in the nonspecific and noncentrosomal categories was usually diffuse, but some probes detected a granular or punctate pattern (2D). These results indicate that a large fraction of expressed genes are localized to centrosomes. They also show that a smaller, but sizable fraction (3−4%) is specifically localized to particular centrosomes.

Centrosomal localization is the most common mode of subcellular localization in this embryo and the focus of these studies. However, we also observed several other notable kinds of RNA localization. One RNA was specifically localized to nuclei, suggesting that it was retained in this

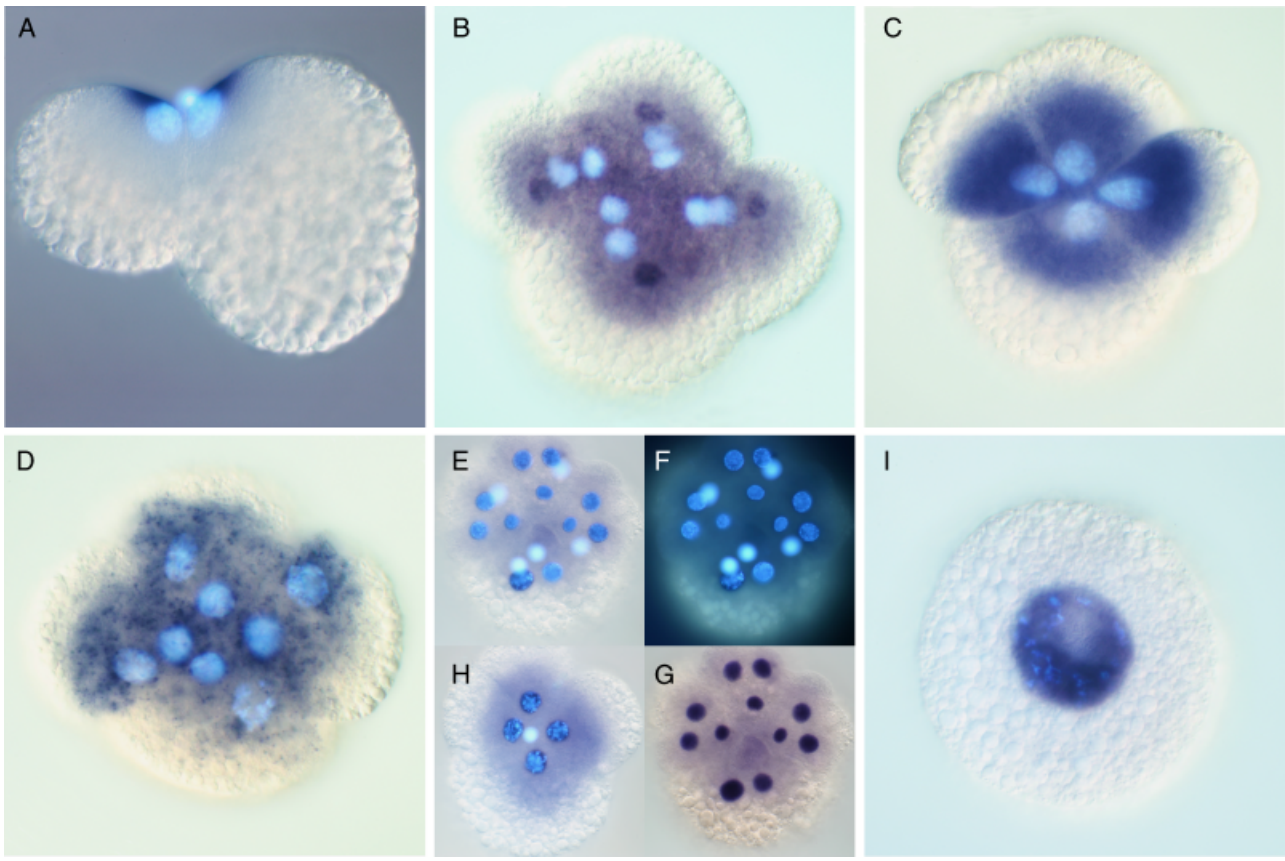

Fig. 2. Kinds of RNA localization in *Ilyanassa*. RNA detected by in situ hybridization is stained with a blue-black chromogenic stain, and the DNA is stained with 4′,6-diamidino-2-phenylindole (DAPI) which is light blue-white in these images. (A) The IoLR5 RNA is specifically localized to the cortex above the nuclei in early prophase of two-cell stage (see also Figure 4D, E and F). (B) The RNA of IoEST056 (no significant homology) is nonspecifically localized to the centrosomes of the macromeres at the eight-cell stage. (C) The RNA of Io α-tubulin-1 is ubiquitous and diffuse in the cytoplasm of the four-cell stage. (D) The mRNA of IoEST051 GCN1-like is ubiquitous in the cytoplasm and granular at the eight-cell stage. (E–H) The RNA of Io Zinc finger 511 is retained in nuclei during early cleavage. (E) DAPI-brightfield merge of a 15–16-cell embryo. (F) DAPI and (G) brightfield of the image shown in (E). The RNA is localized to all nuclei except $1abc^2$ and 1d, which is dividing. (H) Merged image of the same RNA at the four-cell stage in all nuclei. (I) The RNA of the Io cDNA081 (no significant homology) is localized to the germinal vesicle in the oocyte. Scale bars represent 50 μm.

compartment rather than exported to the cytoplasm (Fig. 2, E–G) (Herman et al. 1976; Prasanth et al. 2005). Several RNAs were localized to chromatin during mitosis (data not shown). We did not systematically examine oocytes in this screen, but the mixture of stages in many in situs included unfertilized eggs, and we observed various patterns of localization in the oocyte. Localization to the germinal vesicle was observed for multiple RNAs (e.g., Fig. 2I). These results highlight the general utility of this embryo for examining patterns of subcellular RNA localization.

Specific RNA localization among early blastomeres

To further assess the extent of this mechanism, we sought to identify more specifically localized RNAs. We started a high-throughput in situ screen, where probe synthesis, hybridization, washing, detection, and preliminary visual examination were performed in the 96-well format. We have characterized 18 RNAs from this screen which correspond to specifically centrosomal RNAs. Sequence comparisons among these clones and with the four described above demonstrated that these 18 included 12 additional unique RNAs, bringing the total considered in this study to 16. We named these RNAs according to homology of their coding sequence if present, or IoLR (for *L*ocalized *R*NA; Table 1). We screened 1410 more clones to obtain the additional 18 clones with specific localization. The fraction of specifically localized clones (1.3%) was lower than in the in-depth screen (3–4%), probably because of false negatives in this phase of the screen (see "Materials and Methods" for details).

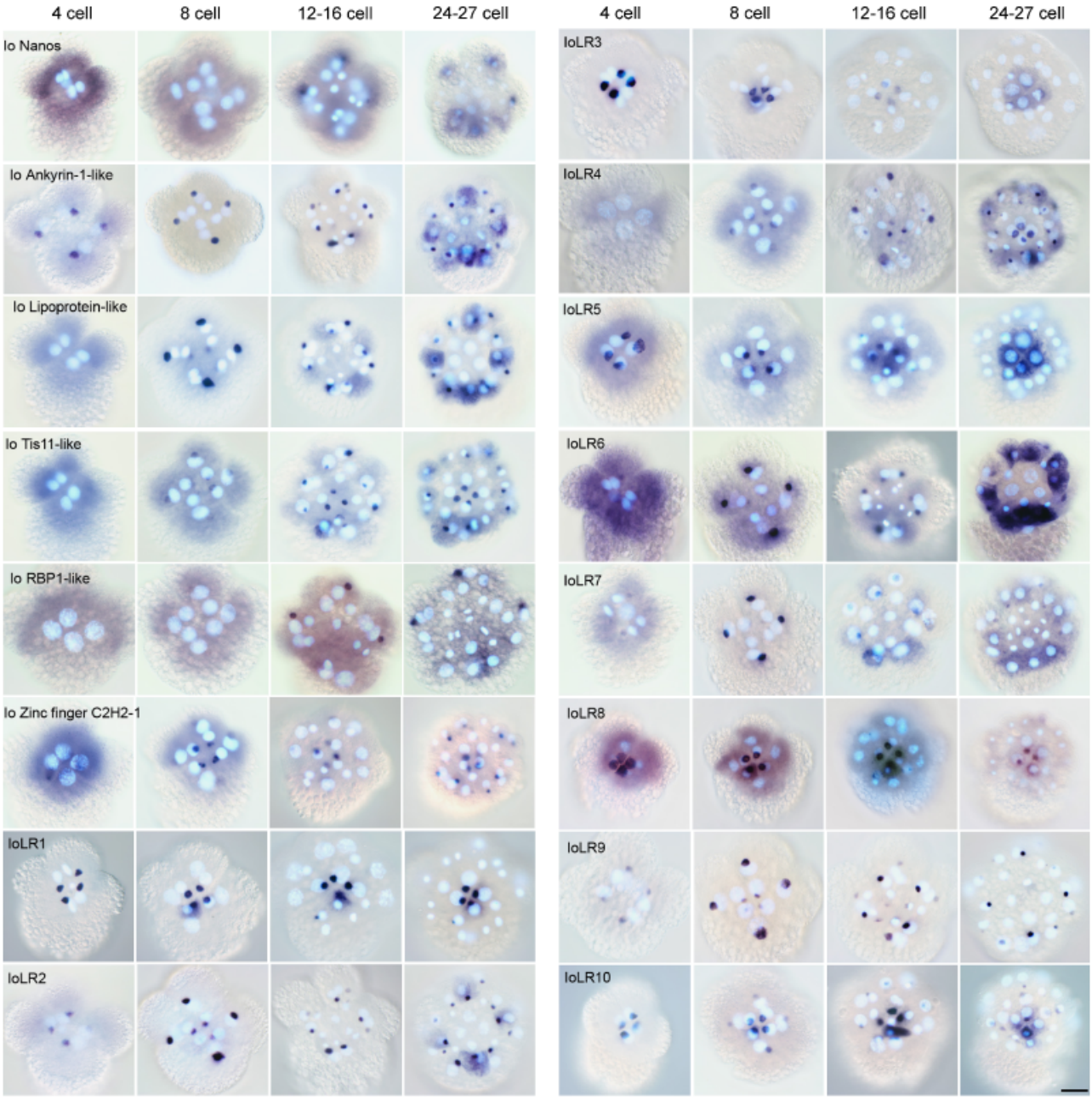

Fig. 3. RNA localization during early cleavage. Patterns of RNA distribution were determined by in situ hybridization for sixteen specifically centrosomal RNAs during early cleavage stages. Stages are indicated at the top, and the name of each RNA is indicated in the first panel of the row of four. RNA is stained with a blue-black chromogenic stain, and the DNA is stained with DAPI which is light blue-white in these merge images. Scale bar represents 50 μm.

Examination of the patterns of distribution of these 16 RNAs shows that centrosomal localization is widespread in the embryo. During the five cleavage stages surveyed here (up to the 24-cell stage), every cell has specific centrosomal localization of at least one RNA (Figs 2 and 3).

Subcellular localization and segregation of localized RNAs

We used fluorescent in situ staining with several different probes to compile a timecourse of localization during the early cleavages. The localization patterns for the IoEven-

Table 1. Kingsley et al. specifically localized RNAs

RNA and clone name	BLAST ID	Blastx E value	Largest ORF (bp)	Clone/contig size (bp)	Genbank Accession
IoNanos[1]	Nanos (CCHC zinc finger)	6.00E-13	1083	2235	EU087572
IoAnkyrin-1[1]	Ankyrin-1	6.00E-24	165	1328	EU087604
IoLipoprotein-like	VsaC lipoprotein	2.00E-16	633	1203	EU087576
IoTis11-like	Zinc finger, Tis11 family (CCCH)	2.00E-36	951	1521	EU087577
IoRBP1	RBP1 (RNA-binding protein-1)	2.00E-23	540	1452	EU087580
Io Zinc finger C2H2-1	Zinc finger protein 135 family (C2H2)	1.00E-31	477	2606	EU087585
IoLR1[1]	nsh	>0.001	441	4222	EU087586
IoLR2[1]	nsh	>0.001	96	433	EU087573
IoLR3	nsh	>0.001	696	1698	EU087571
IoLR4	nsh	>0.001	168	653	EU087575
IoLR5	nsh	>0.001	429	2055	EU087578
IoLR6	nsh	>0.001	396	1206	EU087584
IoLR7	nsh	>0.001	573	1045	EU087583
IoLR8	nsh	>0.001	165	783	EU087582
IoLR9	nsh	>0.001	225	1451	EU087581
IoLR10	nsh	>0.001	249	809	EU087579

Notes:
[1]Found in the initial screen.
nsh, no significant homology; ORF, open reading frame.

Fig. 4. Subcellular localization of several specifically localized RNAs during early cleavage stages. The RNA is localized by in situ hybridization detected with fluorescent tyramide precipitation (red). DNA is stained with 4′,6-diamidino-2-phenylindole DAPI, (blue). Microtubules are stained with an antibody against β-tubulin (green). Images are projections of confocal Z-stacks. Yellow indicates that RNA and microtubules are colocalized, or superimposed in different sections. (A) Zygote just before fusion of female (left) and male (right) pronuclei. Two foci of IoLR5 RNA staining are observed, one is over the female pronucleus and thus appears magenta. The upper-most optical sections containing the polar bodies were omitted for clarity. (B) Metaphase of the first division. The IoLR5 RNA is diffuse around the spindle. (C) At telophase of the first division, IoLR5 RNA is localized to the broadly shaped spindle poles. (D) At the two-cell interphase, the IoLR5 RNA is localized to spherical centrosomes adjacent to the nuclei. (E) At the two-cell prophase, the IoLR5 RNA is moving the cortex, and the prophase asters are visible as two foci in each cell, under the RNA. (F) In the metaphase of the second cleavage, the IoLR5 RNA is localized to a patch on the cortex of each dividing cell. (G) At cytokinesis of the second cleavage, the IoLR5 RNA is localized to the spindle poles, adjacent to the nuclei. (H) At interphase of the four-cell stage, the IoLR5 RNA is localized to the centrosomes in each cell. At prophase (I) and metaphase (J) of the third cleavage, the IoLR1 RNA is localized to the cortex and the asters are visible. (K) At telophase of the third cleavage, the IoLR1 RNA is on the cortex in the first quartet micromeres. (L) During cytokinesis of the third cleavage cycle, the IoLR2 RNA surrounds the spindle poles in the macromeres. (M) At the interphase-prophase transition of the eight-cell stage, two macromeres are in interphase (1A and 1B, left and top) and show IoLR2 RNA localization to the large spherical centrosomes. The other two are in prophase: at this stage the RNA is moving from the centrosomes to the cortex and the prophase asters are visible as two small foci of microtubules under the RNA in 1D (lower macromere). (N) In metaphase of the fourth division, the IoLR2 RNA is on the cortex in all cells, and the spindles are aligned toward the RNA, which changes from a disk-shaped patch to a ring, with the spindle pole at its center. (O) During cytokinesis of the fourth division, the IoLR2 RNA is on the cortex of the second quartet micromeres. (P) At the 12–15-cell stage, the IoTis11-like RNA is accumulating on the macromere centrosomes. Large midbodies are observed between the macromeres and the second quartet cells. (Q) At the 15–16-cell stage, the D macromere (bottom) is in prophase, with the IoTis11-like RNA on the cortex, and the RNA is on the centrosome in the other macromeres. Weaker centrosomal localization is also observed in 1abc[1] and 2abcd[2]. (R) At the 16-cell prophase, the IoTis11 RNA is cortical in the macromeres. (S) At the fifth cleavage cycle the IoTis11-like RNA is in cortical ring-shaped patches in the third quartet micromeres. Asymmetric segregation can also be observed in the dividing second quartet cells. The RNA is centrosomal in 1abcd[1] and 1abcd[2]. (T) At the 24-cell stage, the IoTis11-like RNA is centrosomal in most micromeres. All confocal images are from the animal pole, with the D quadrant down, where applicable. Different apparent sizes of the embryos are due to different amounts of compression before imaging, and different depths of Z-sectioning. In some embryos, the yolk granules are weakly autofluorescent in the green channel. One to two polar bodies are visible in some images, but they are frequently lost during processing. (U) Schematic diagram summarizing the relationship of the localized RNA to the centrosome during macromere cleavage cycles. RNA (red) moves to the centrosome during cytokinesis. During prophase, the RNA moves to the cortex of the cell and the prophase asters are visible. The spindle aligns to the patch of RNA on the cortex, and the RNA is inherited by one daughter cell. Another RNA (yellow) is localized to the macromere centrosome in the next interphase.

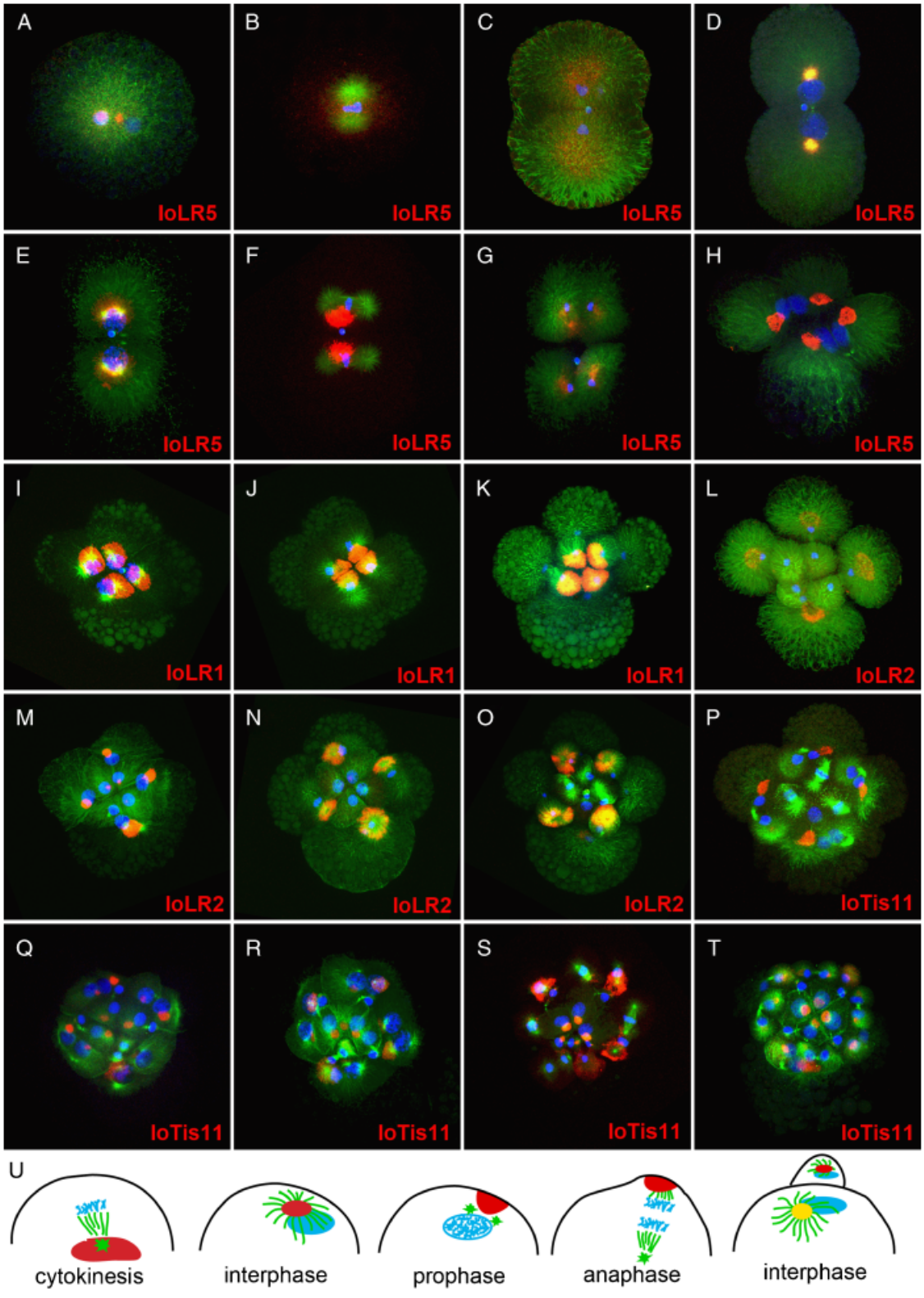
A
IoLR5
B
IoLR5
C
IoLR5
D
IoLR5
E
IoLR5
F
IoLR5
G
IoLR5
H
IoLR5
I
IoLR1
J
IoLR1
K
IoLR1
L
IoLR2
M
IoLR2
N
IoLR2
O
IoLR2
P
IoTis11
Q
IoTis11
R
IoTis11
S
IoTis11
T
IoTis11
U
cytokinesis
interphase
prophase
anaphase
interphase

skipped mRNA during the third cleavage cycle have been reported (Lambert and Nagy 2002); here we document the localization and movement of RNAs from the zygote to the 24-cell stage. The four probes that were used for these stages are indicated in the Fig. 4 legend. In general, this timecourse shows that the behavior of localized RNAs in the macromeres, before segregation to the micromeres, is similar between different cleavage cycles. In the macromeres, the movement of RNAs to the centrosome occurs during the completion of each division (in telophase and cytokinesis). The RNAs that go to the macromere centrosomes in each cell cycle are diffuse in the cytoplasm in the previous cycle (Fig. 3, e.g., IoLipoprotein-like mRNA and IoLR7, and Fig. 4, B and C). The exception is the IoLR5 RNA at the four-cell stage, which is localized to the cortex during the second cleavage, and moves to the centrosomes from the cortex rather than from a diffuse distribution in the cytoplasm (Fig. 4, F and G).

During interphase, localized RNAs are found on the large spheroid centrosomes near the nuclei (Fig. 4, D, H, M, Q and T). During prophase, the RNA moves to the cell cortex (Fig. 4, E, F, I, M and R). At the two-cell prophase, the RNA moves across the animal side of each nucleus, to a location very near the animal-most part of the first cleavage furrow (Fig. 4, E and F). Similarly, at the four-cell prophase, the RNA moves from the centrosome at the vegetal side of the nuclei to the cortex at the animal side, very near the animal pole of the embryo (compare Fig. 4, H and I). In the fourth and fifth macromere cell cycles, the RNA apparently moves more directly to the cortex, localizing to the region of the cortex that overlies the interphase centrosome (Fig. 4, M, R and S). However, even in these cases, the RNA seems to divert slightly toward to the animal pole as it moves to the cortex. In all cases, the prophase asters are observed first between the nucleus and the RNA-containing centrosomal material, as this component moves to the cortex (Fig. 4, E, I, M and R). All observed RNA segregation in the macromere divisions is toward the animal pole, to the daughter micromeres, as described above. However, when the micromeres divided, the segregation could be toward the animal or vegetal pole (e.g., Fig. 4S and data not shown).

Patterns of localized mRNAs

Regardless of the large fraction of RNAs that are localized, the potential contribution of this mechanism to patterning depends on the diversity of different patterns that it can generate. Remarkably, 15 of the 16 specifically localized patterns were unique, when compared across all stages using the summary notation in Fig. 5. This is conservative, because the summary ignores some differences between RNA patterns, such as differences between cells in a quartet, and differences in the distribution of unlocalized RNA in the embryo. Similarly, 19 of the 48 nonspecifically centrosomal RNAs also have unique patterns of localization across early cleavage stages. Even though the patterns are highly diverse, there are several recognizable families of patterns, which may reflect similarities in the mechanisms of localization of these RNAs. For instance, four of the localized RNAs have very similar localization in the first quartet lineages (Fig. 5; IoLR1, IoLR3, IoLR5, and IoLR8).

The last time-point in our screen, the 24–27-cell stage, is an important interval. At this stage, differences in developmental potential have been established between the three quartets of micromeres. These differences determine the responses of cells to the embryonic organizer, which begins signaling at this stage (Sweet 1998; Lambert and Nagy 2001). Therefore, the diversity of patterns of RNA localization at this stage is particularly important; moreover, it is possible for two RNAs to have different patterns of localization when compared across all stages, but be identical at the 24–27-cell stage. Among specifically centrosomal RNAs, there were 10 different patterns at the 24-cell stage, based on our summary in Fig. 5. These results show that the mechanisms of localization in *Ilyanassa* are highly intricate; there are a large number of RNAs localized in many different patterns.

Segregation after localization

We often observed specifically centrosomal RNAs being asymmetrically segregated during mitosis, and have observed segregation in all divisions from the 4–24-cell stages with at least one RNA (Fig. 4 and data not shown). However, we also wanted to estimate the overall rates of segregation of specifically centrosomal RNAs, using the patterns of localization as summarized in Fig. 5. For each instance of specific localization in a set of cells (M, 1q, 1M, 2q, 2M) whose daughters we examined in our screen, we scored whether the RNA was enriched in one daughter cell of a division, consistent with segregation.

Specific localization often leads to enrichment in daughter cells in the ensuing division. In the macromere divisions, where segregation is always into the micromere daughter, 27 of 31 cases have enrichment in the micromere. In the divisions of first and second quartet micromeres, eight of 21 divisions result in enrichment in one daughter, consistent with segregation. As there is evidence for mRNA transcription in *Ilyanassa* as early as the four-cell stage (Collier 1975), it is possible that some of enrichment in the daughter cells examined arises de novo. This appears to be rare: of the 79 cases where we observed enrichment in a micromere, in only four was it not explicable by localization in the mother cell. These were the first quartet localization in IoLipoprotein-like, IoLR4, IoTis11-like, and the third quartet localization of Io Zinc finger C2H2-1. Conversely, in some of the cases where we do not see enrichment in the following division, it is

possible that the RNA is segregated, but that it is degraded in the cells that inherit it.

Among RNAs that were nonspecifically localized to macromere centrosomes, in 33 of 90 cases there was localization to the daughter micromere in the next division, suggesting segregation. In micromeres, 10 of 20 cases of nonspecific localization were enriched in one daughter cell in the next division.

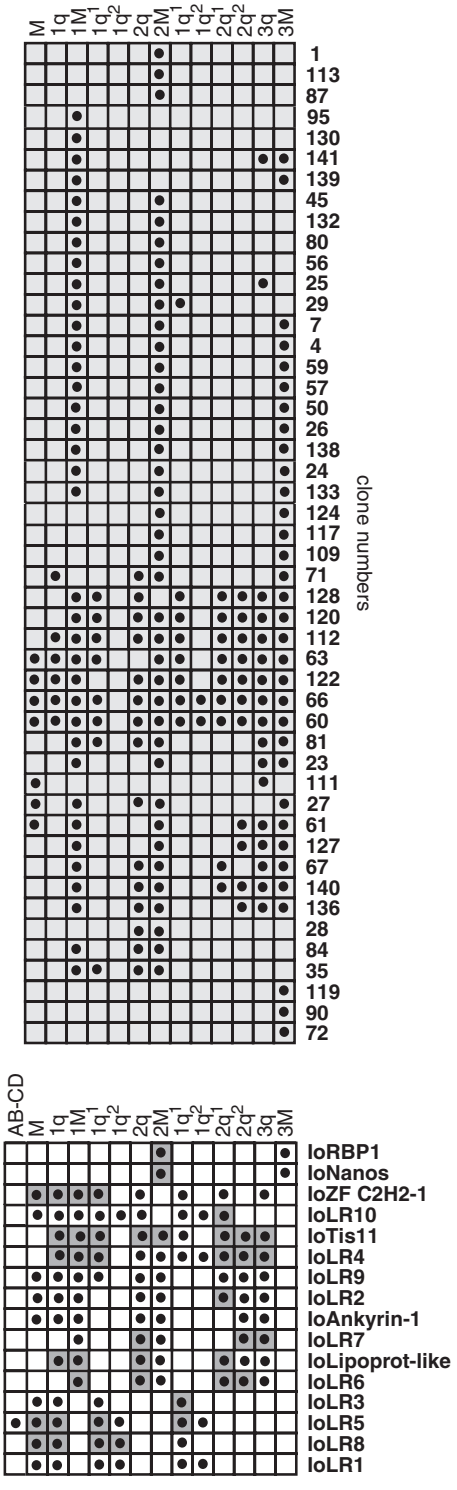

Predicted functions of centrosomal RNAs

A previous study found that mRNAs for three developmental regulatory proteins (*Ilyanassa* Even-skipped, Decapentaplegic and Tolloid) were specifically localized to centrosomes, but the mRNA for the 40S ribosomal protein S3a was not (Lambert and Nagy 2002). This raised the possibility that genes involved with embryonic patterning were preferentially localized to centrosomes, which is intuitively appealing since these RNAs are being segregated like determinants. In order to ask what kinds of RNAs are centrosomally localized, we assigned putative functions based on BLAST searching and protein motif searches (see "Materials and Methods").

About half of the initial set of RNAs had significant sequence homology in BLAST searches, using an E value of 0.001 as a cut-off (Table 1, Fig. S1). Of the 16 specifically centrosomal RNAs, six had significant homology (Table 1). The predicted functions of the nonspecifically centrosomal RNAs were not appreciably different from the predicted functions of the unlocalized RNAs. Both sets included mRNAs for many structural and core metabolic proteins, as well as a few molecules that could have regulatory roles. Neither set of RNAs contained orthologs of canonical developmental patterning molecules. There were two potential transcription factor proteins among the nonspecifically centrosomal RNAs. One was a C2H2 zinc finger protein

Fig. 5. Summary of centrosomal RNA localization patterns. The patterns of the nonspecifically localized RNAs (top panel) and specifically localized RNA (bottom panel) were summarized by scoring the sets of cells where localization was observed. Specific centrosomal localization is indicated with a circle against a white background, and nonspecific localization is indicated with a circle against a gray background. As we define specifically localized RNAs as those with specifically centrosomal localization in at least one set of cells at one stage, many specifically localized RNAs are non-specifically localized in some cells. The sets of cells are indicated at the top of each chart, and defined as follows. AB−CD indicates the two cells of the two-cell stage (lower panel only). M is the four-cell stage macromeres. 1M are the eight-cell stage macromeres, and 1q are the first quartet micromeres. At the 12−16-cell stage, 2M are the macromeres, 2q are the second quartet, and $1q^1$ and $1q^2$ are the daughters of the first quartet. At the 24-cell stage, 3M are the macromeres, 3q are the third quartet, $2q^1$ and $2q^2$ are the daughters of the second quartet. The second instances of $1q^1$ and $1q^2$ indicate localization in these cells at the 24-cell stage. The clone numbers or names are indicated on the right side of the charts. As most but not all localization was quadrilaterally symmetrical (i.e., in all four macromeres or all four cells of a given quartet of micromeres), this summary is a conservative estimate of the diversity and disparity of patterns.

(IoEST130), and the other was a MAX-related bHLH protein (IoEST057).

Of the six specifically localized RNAs with significant homology, three encode zinc finger motifs. There are many different classes of zinc finger motifs, with diverse structures and predicted functions. Each of the three zinc finger-containing RNAs recovered represents a different class of zinc finger motif (Table 1), and all three classes contain representatives that are known to bind nucleic acids (Kersey et al. 2005). The localized IoNanos RNA encodes an *Ilyanassa* ortholog of the Nanos protein, which contains a CCHC zinc finger and has conserved roles in germline specification and embryonic patterning (Wang and Lehmann 1991; Tsuda et al. 2003; Agee et al. 2006). IoTis11-like and Io Zinc finger C2H2-1 RNAs contain CCCH and C2H2 class zinc fingers, respectively. Representatives of these classes are also involved in early patterning and cell fate specification in other systems (Rosenberg et al., 1986; Guedes and Priess, 1997). Another specifically centrosomal RNA encodes an RNA recognition motif (RRM), with highest similarity to the conserved splicing factor *D. melanogaster* RBP1, which is involved in splicing activation and splice site selection in the sex determination pathway (Heinrichs and Baker, 1995). When the zinc finger proteins are taken together with this splicing factor, four of our six identifiable specifically centrosomal RNAs are homologous to nucleic acid binding proteins with regulatory roles in other systems.

DISCUSSION

The data presented here demonstrate the existence of an extensive machinery for RNA segregation during early cleavage of a spiralian embryo. A relatively large fraction of RNAs are specifically localized to centrosomes in these cells, and all of the cells in the early embryo have specific RNA localization. Perhaps most importantly, these mechanisms of RNA localization generate a large diversity of patterns in the blastula. Together, these results show that RNA segregation is widespread in the *Ilyanassa* embryo and common among embryonic transcripts. An obvious implication of these results is that specification of many cell fates in early mollusc development involves the segregation of determinant RNAs. Consistent with this, we found that a significant portion of specifically localized RNAs encode proteins homologous to nucleic acid binding factors with regulatory functions in other systems.

Recent findings, especially in *Caenorhabditis elegans* and ascidians, have led to the abandonment of the mosaic *versus* regulative dichotomy in the description of animal embryos. Although *Ilyanassa* is clearly not a purely mosaic embryo, our data highlight the fact that there is a continuum in the relative importance of autonomous cues in early cell fate specification among animal embryos. In light of these results, we revisit the concept of mosaic development below.

RNA localization in *Ilyanassa*

Specific RNA localization was observed in all cells in early cleavage stages. In most divisions, one or more specifically centrosomal RNAs were segregated asymmetrically. The exceptions are the divisions in the second cleavage cycle, when the two cells AB and CD divide. When AB divides, RNA that is specifically centrosomal is partitioned equally between the two daughter cells. This is consistent with what is known about the developmental potential of these two cells, which are thought to be equivalent based on existing embryological studies. For instance, AD and BD half-embryos develop similarly, and 1a and 1b behave similarly in transplantation assays (McCain and Cather 1989; Sweet 1998). Centrosomal RNA is also segregated symmetrically in the division of CD. In this case, the daughter cells C and D have very different potentials because the D cell inherits the polar lobe in the first two divisions, which gives the D lineage a special cleavage pattern and the role of organizer after the fifth cleavage cycle (Crampton 1896; Clement 1952; Clement 1962). The polar lobe is a classic example of segregation of cytoplasmic determinants, and so would seem to be a likely site for localized RNA. We have not yet found any RNAs that are localized to the polar lobe.

There are general differences in patterns of localization between quartets. We found four RNAs that were specifically localized to the cells of the first quartet, and all of these RNAs conform to a simple mode of localization. They were all localized to the four-cell macromere centrosomes and then inherited by the first quartet cells. They were not subsequently localized in the macromeres or in the later quartets (IoLRs 1, 3, 5, 8). This simple pattern did not hold for the second and third quartets. For RNAs that become restricted to the second quartet, there was always localization to the eight-cell stage macromeres (as expected), but this was followed by localization to the 16-cell macromeres and the third quartet micromeres. In these cases, the RNA in the third quartet cells is less abundant and often remains centrosomal when the second quartet RNA populations become cytoplasmic. For several of these RNAs we have determined that the pattern becomes specific to the second quartet in later stages, by decay in the third quartet cells (J. D. Lambert and X. Chan, unpublished observations). Specific localization to the third quartet is also attained in a more complex fashion than localization to the first quartet. The RNAs that are ultimately specific to the third quartet are initially localized in other cells as well, and become restricted to the third quartet lineages by RNA decay in other lineages. This is true of the IoDpp mRNA (Lambert and Nagy 2002), and two other RNAs from this screen (IoLR4 and IoTis11-like; J. D. Lambert and

X. Chan, unpublished observations). In general, it appears that localization to the first quartet can be accomplished directly by asymmetric segregation, but specific localization to the second and third quartets is attained by RNA segregation along with elimination of RNA in some lineages.

The distribution of localized RNAs along the secondary axis

Between the four-cell stage and the 24-cell stage, the patterns of localization that we observe are almost all radially symmetrical around the animal-vegetal axis, i.e., localization is found in corresponding cells in all four quadrants, like the four micromeres in a quartet. As expected, the only exceptions to this involve the D quadrant, which is known to differ from the others based on the inheritance of the polar lobe (Clement 1952; Sweet 1998; Goulding 2003). However, these differences are subtle; for instance, we have not found any RNA that is specific to the D quadrant, or specifically excluded from it. It is notable that the 1d cell has a patch of cortex that binds several RNAs during interphase, when other cells in this quartet only have localization to the centrosome (see Fig. 3, eight-cell stage panels of IoLR1 and IoLR3). After the onset of organizer signaling at the 24-cell stage, the patterns of most RNAs we have examined do begin to differ depending on the location along the secondary axis (X. Y. Chan and J. D. Lambert, unpublished observations), probably in response to organizer signaling.

The identity of localized RNAs

We can identify six of the sixteen specifically localized RNAs found in this screen. Of these six, one encodes an ankyrin-1-like protein and one contains a putative lipoprotein motif. The remaining four encode proteins with homology to nucleic acid-binding factors with regulatory roles in other systems. This finding is consistent with this class of RNA being enriched for transcripts involved in transcriptional or translational regulation.

The fraction of specifically centrosomal RNAs that are identifiable is similar to the fraction in our initial survey (37% and 50%, respectively). Several effects are likely contributing to the frequency of unidentifiable RNAs, including incomplete cDNAs, and open reading frames without clear homology to proteins in other systems. It is also important to note that these RNAs could be noncoding RNAs, which are not uncommon in metazoan transcriptomes (Carninci et al. 2005; Inagaki et al. 2005; Tupy et al. 2005).

The finding that a large fraction of the specifically localized RNAs encode zinc finger motifs has a parallel in the early *C. elegans* embryo. In this system two proteins with patterning roles, PIE-1 and MEX-5, are localized to centrosomes (Reese et al. 2000; Schubert et al. 2000). Intriguingly, both of these centrosomally localized patterning proteins contain CCCH zinc-finger domains, like IoTis11-like. Of course, it remains to be seen if the IoTis-11 protein is localized to centrosomes.

Asymmetric cell division in metazoan embryos: the mosaic embryo revisited

We have shown that asymmetric segregation is exceptionally widespread in the early *Ilyanassa* embryo, both in terms of lineages and the number of RNAs that are involved. This suggests that *Ilyanassa* is extensively patterned by segregation of determinants during early cleavages. Such events will probably not specify cell fates autonomously in most lineages. This is because specification of most cells in the blastula requires induction from the embryonic organizer, 3D (Clement 1962; Sweet 1998; Lambert and Nagy 2001). In our working model, the role of most asymmetric cell division in the early embryo is to imbue different groups of cells with different responses to the inductive signals from 3D. The existence of such differences has been shown experimentally (Sweet 1998). The requirement for segregated determinants for various lineages will have to be tested in a molecule-by-molecule approach.

Ilyanassa seems to have high levels of RNA localization and segregation relative to other embryos, but comparisons with analyses in other systems are somewhat confounded by differences in the cell biology of other embryos and experimental designs (Seydoux and Fire 1994; Tabara et al. 1996; Kudoh et al. 2001; Tomancak et al. 2002). The embryos which seem to be most similar to *Ilyanassa* in the level of RNA localization and segregation are those of ascidians. In *Halocynthia roretzi* 3.5% of RNAs examined were localized to regions in the posterior blastomeres called the postplasm (Makabe et al. 2001). There was also subcellular localization of some RNAs in anterior blastomeres, although the frequency of subcellular localization in these cells was not measured explicitly. At least some postplasmic RNAs are segregated in the germline during division (Yoshida et al. 1996; Nishida and Sawada 2001; Nakamura et al. 2006). Thus, the available data suggest that the fraction of RNAs that are subcellularly localized is similar between ascidian and mollusc embryos, but that in *Ilyanassa,* localization and segregation occurs in more lineages of the embryo.

Mosaic development is a simplistic term that refers to idealized embryos where all cell specification is driven by autonomous cues, like segregated determinants. Mollusc and ascidian embryos are classic examples of mosaic development. Traditionally, mosaic development is contrasted with regulative development, where fates are specified conditionally. As has been noted, our current knowledge of early embryonic patterning makes the regulative versus mosaic dichotomy untenable because all animal embryos examined thus far develop using a combination of conditional and autonomous

specification. Even the embryos that seemed most likely to be dominated by autonomous specification—including molluscs, ascidians, nematodes, and ctenophores—are now known to depend heavily on inductive interactions (Clement 1962; Cather 1971; Goldstein 1992; Martindale and Henry 1997; Henry and Martindale 2001; Lambert and Nagy 2001; Nishida 2005; Lawrence and Levine 2006). It is clearly not possible to infer autonomous specification from the observation of a highly stereotyped cleavage pattern; the latter may be necessary to position cells for cellular interactions (Martindale and Henry 1997; Bischoff and Schnabel 2006).

Although there are no purely mosaic or purely regulative embryos, there are basic differences in how animal embryos work. These differences are important because they expand our knowledge of the range of extant patterning mechanisms, and inform understanding of how embryonic patterning evolves. The finding that all lineages in the early *Ilyanassa* embryo are characterized by segregation of RNAs has implications for understanding the extremely conservative nature of spiralian development. Although most animal phyla have idiosyncratic modes of early development, the several phyla with spiralian development have remarkable similarities in the pattern of cleavages, the fate map, and the patterning mechanisms of the early embryo (Wilson 1899; Henry and Martindale 1999). One possible explanation for this unusual level of interphyletic conservation is that the spiralian embryo is particularly reliant on autonomous cues, and that this dependence puts interlocking constraints on both cleavage pattern and cell fate specification.

Acknowledgments

We thank Jeremy Rabinowitz for helpful discussions throughout the course of the work, as well as advice on the manuscript; Morgan Goulding for careful and critical reading of the manuscript; and the Developmental Studies Hybridoma Bank for making the β-tubulin antibody available. This work was supported in part by an NSF grant (0544220) to J. D. L.

REFERENCES

Agee, S. J., Lyons, D. C., and Weisblat, D. A. 2006. Maternal expression of a NANOS homolog is required for early development of the leech *Helobdella robusta*. *Dev. Biol.* 298: 1–11.

Altschul, S. F., Gish, W., Miller, W., Myers, E. W., and Lipman, D. J. 1990. Basic local alignment search tool. *J. Mol. Biol.* 215: 403–410.

Bischoff, M., and Schnabel, R. 2006. Global cell sorting is mediated by local cell-cell interactions in the *C. Elegans*. *Dev. Biol.* 294: 432–444.

Carninci, P., et al. 2005. The transcriptional landscape of the mammalian genome. *Science* 309: 1559–1563.

Cather, J. N. 1971. Cellular interactions in the regulation of development in annelids and molluscs. *Adv. Morphol.* 9: 67–125.

Clement, A. C. 1952. Experimental studies on germinal localization in *Ilyanassa*. I. The role of the polar lobe in determination of the cleavage pattern and its influence in later development. *J. Exp. Zool.* 132: 427–446.

Clement, A. C. 1962. Development of *Ilyanassa* following the removal of the D macromere at successive cleavage stages. *J. Exp. Zool.* 149: 193–216.

Collier, J. R. 1975. Polyadenylation of nascent RNA during embryogenesis of *Ilyanassa obsoleta*. *Exp. Cell Res.* 95: 263–268.

Collier, J. R. 1981. Methods of obtaining and handling eggs and embryos of the marine mud snail *Ilyanassa obsoleta*. In National Resource Council (U.S.) (ed.). *Laboratory Animal Management: Marine Invertebrates*. National Academy Press, Washington, DC, 217–232.

Crampton, H. E. 1896. Experimental studies on gastropod development. *Roux' Arch. Entw.-mech* 3: 1–19.

Goldstein, B. 1992. Induction of gut in *Caenorhabditis elegans* embryos. *Nature* 357: 255–257.

Goulding, M. 2003. Cell contact-dependent positioning of the D cleavage plane restricts eye development in the *Ilyanassa* embryo. *Development* 130: 1181–1191.

Guedes, S., and Priess, J. R. 1997. The *C. elegans* MEX-1 protein is present in germline blastomeres and is a P granule component. *Development* 124: 731–739.

Heinrichs, V., and Baker, B. S. 1995. The *Drosophila* SR Protein RBP1 contributes to the regulation of doublesex alternative splicing by recognizing RBP1 RNA target sequences. *EMBO J.* 14: 3987–4000.

Henry, J. J., and Martindale, M. Q. 1999. Conservation and innovation in spiralian development. *Hydrobiologia* 402: 255–265.

Henry, J. Q., and Martindale, M. Q. 2001. Multiple inductive signals are involved in the development of the ctenophore *Mnemiopsis leidyi*. *Dev. Biol.* 238: 40–46.

Herman, R. C., Williams, J. G., and Penman, S. 1976. Message and non-message sequences adjacent to poly(A) in steady-state heterogeneous nuclear RNA of hela-cells. *Cell* 7: 429–437.

Inagaki, S., et al. 2005. Identification and expression analysis of putative mrna-like non-coding RNA in *Drosophila*. *Genes to Cells* 10: 1163–1173.

Kersey, P., et al. 2005. Integr8 and Genome Reviews: integrated views of complete genomes and proteomes. *Nucleic Acids Res.* 33: D297–302.

Kudoh, T., et al. 2001. A gene expression screen in zebrafish embryogenesis. *Genome Res.* 11: 1979–1987.

Lambert, J. D., and Nagy, L. M. 2001. MAPK signaling by the D quadrant embryonic organizer of the mollusc *Ilyanassa obsoleta*. *Development* 128: 45–56.

Lambert, J. D., and Nagy, L. M. 2002. Asymmetric inheritance of centrosomally localized mrnas during embryonic cleavages. *Nature* 420: 682–686.

Lawrence, P. A., and Levine, M. 2006. Mosaic and regulative development: two faces of one coin. *Curr. Biol.* 16: R236–R239.

Makabe, K. W., et al. 2001. Large-scale cdna analysis of the maternal genetic information in the egg of *Halocynthia roretzi* for a gene expression catalog of ascidian development. *Development* 128: 2555–2567.

Martindale, M. Q., and Henry, J. Q. 1997. Reassessing embryogenesis in the Ctenophora: the inductive role of e1 micromeres in organizing ctene row formation in the 'mosaic' embryo, *Mnemiopsis leidyi*. *Development* 124: 1999–2006.

McCain, E. R., and Cather, J. N. 1989. Regulative and mosaic development of *Ilyanassa obsoleta* embryos lacking the A-quadrant and C-quadrant. *Invertebr. Reprod. Dev.* 15: 185–192.

Nakamura, Y., Makabe, K. W., and Nishida, H. 2006. The functional analysis of Type I postplasmic/PEM mrnas in embryos of the ascidian *Halocynthia roretzi*. *Dev. Genes. Evol.* 216: 69–80.

Nishida, H. 2005. Specification of embryonic axis and mosaic development in ascidians. *Dev. Dyn.* 233: 1177–1193.

Nishida, H., and Sawada, K. 2001. Macho-1 encodes a localized mRNA in ascidian eggs that specifies muscle fate during embryogenesis. *Nature* 409: 724–729.

Prasanth, K. V., et al. 2005. Regulating gene expression through RNA nuclear retention. *Cell* 123: 249–263.

Reese, K. J., Dunn, M. A., Waddle, J. A., and Seydoux, G. 2000. Asymmetric segregation of PIE-1 in C-elegans is mediated by two complementary mechanisms that act through separate PIE-1 protein domains. *Mol. Cell* 6: 445–455.

Rosenberg, U. B., et al. 1986. Structural homology of the product of *Drosophila* kruppel gene with *Xenopus* Transcription Factor-IIIA. *Nature* 319: 336−339.

Schubert, C. M., Lin, R. L., de Vries, C. J., Plasterk, R. H. A., and Priess, J. R. 2000. MEX-5 and MEX-6 function to establish soma/germline asymmetry in early *C. Elegans embroys*. *Mol. Cell* 5: 671−682.

Seydoux, G., and Fire, A. 1994. Soma-germline asymmetry in the distributions of embryonic rnas in *Caenorhabditis elegans*. *Development* 120: 2823−2834.

Sweet, H. C. 1998. Specification of first quartet micromeres in *Ilyanassa* involves inherited factors and position with respect to the inducing D macromere. *Development* 125: 4033−4044.

Tabara, H., Motohashi, T., and Kohara, Y. 1996. A multi-well version of *in situ* hybridization on whole mount embryos of *Caenorhabditis elegans*. *Nucleic Acids Res*. 24: 2119−2124.

Tomancak, P, et al. 2002. Systematic determination of patterns of gene expression during *Drosophila* embryogenesis. *Genome Biol*. 3, research0088.1−0088.14.

Tsuda, M., et al. 2003. Conserved role of nanos proteins in germ cell development. *Science* 301: 1239−1241.

Tupy, J. L., et al. 2005. Identification of putative noncoding polyadenylated transcripts in *Drosophila melanogaster*. *Proc. Natl. Acad. Sci. USA* 102: 5495−5500.

Wang, C., and Lehmann, R. 1991. Nanos is the localized posterior determinant in *Drosophila*. *Cell* 66: 637−647.

Wilson, E. B. 1899. Cell-lineage and ancestral reminiscence. In *Biological Lectures 1898; The Marine Biological Laboratory, Wood's Holl, Mass*. The Athenaeum Press, Boston.

Wilson, E. B. 1904. Experimental studies in germinal localization. II Experiments on the cleavage-mosaic in *Patella* and *Dentalium*. *J. Exp. Zool*. 1: 197−268.

Yoshida, S., Marikawa, Y., and Satoh, N. 1996. Posterior end mark, a novel maternal gene encoding a localized factor in the ascidian embryo. *Development* 122: 2005−2012.

Zdobnov, E. M., and Apweiler, R. 2001. Interproscan—an integration platform for the signature-recognition methods in interpro. *Bioinformatics* 17: 847−848.

SUPPLEMENTARY MATERIAL

The following material is available for this article online:

Table S1.

This material is available as part of the online article from: http://www.blackwell-synergy.com/doi/abs/10.1111/j.1525-142X.2007.00194.x (This link will take you to the article abstract).

Please note: Blackwell Publishing are not responsible for the content or functionality of any supplementary materials supplied by the authors. Any queries (other than missing material) should be directed to the corresponding author for the article.